



Published in final edited form as:

Mol Ther. 2008 January ; 16(1): 146–153. doi:10.1038/sj.mt.6300343.

Exponential Enhancement of Oncolytic VSV Potency by Vector-Mediated Suppression of Inflammatory Responses In Vivo

Jennifer Altomonte^{1,4}, Lan Wu¹, Li Chen¹, Marcia Meseck¹, Oliver Ebert^{1,4}, Adolfo García-Sastre², John Fallon³, and Savio L.C. Woo¹

¹Department of Gene and Cell Medicine, Mount Sinai School of Medicine, New York, NY 10029, USA

²Department of Microbiology, Mount Sinai School of Medicine, New York, NY 10029, USA

³Department of Pathology, Mount Sinai School of Medicine, New York, NY 10029, USA

Abstract

Oncolytic virotherapy is a promising strategy for treatment of malignancy, although its effectiveness is hampered by host anti-viral inflammatory responses. Indeed the treatment efficacy of oncolytic Vesicular Stomatitis Virus (VSV) in rats bearing multi-focal Hepatocellular Carcinoma (HCC) can be substantially elevated by antibody-mediated depletion of NK cells. To test the hypothesis that the oncolytic potency of VSV could be exponentially elevated by evading inflammatory responses in vivo, we constructed a recombinant VSV vector expressing equine herpesvirus-1 glycoprotein G, which is a broad-spectrum viral chemokine binding protein (rVSV-gG). Hepatic artery infusion of rVSV-gG in immune-competent rats bearing syngeneic and multi-focal HCC in the livers resulted in a reduction of NK and NKT cells in the tumors and a one-log enhancement of intratumoral virus titer over a reference rVSV vector. The treatment led to elevated tumor necrosis and substantially prolonged animal survival without toxicities. These results indicate that rVSV-gG could be developed as an effective and safe oncolytic agent to treat advanced HCC patients in the future. Furthermore, the novel concept that oncolytic potency can be substantially enhanced by vector-mediated suppression of host anti-viral inflammatory responses might have general applicability in the field of oncolytic virotherapy for cancer.

Keywords

oncolytic virotherapy; liver cancer; inflammatory response; recombinant VSV; viral chemokine binding protein

INTRODUCTION

Oncolytic viruses have emerged as attractive therapeutic agents for cancer treatment due to their selective ability to replicate and kill tumor cells in vitro and in vivo.^{7–10} VSV, a member of the *Rhabdoviridae* family, is a particularly attractive oncolytic agent because of its short replication cycle and ability to reach high titers in most rodent and human tumor cells. It is an enveloped, negative-strand RNA virus that has a wide host range, but replicates selectively within tumor cells due to defects in anti-viral type I interferon responses in these cells.¹¹ While the natural hosts for VSV infection are cattle, horses and pigs, infections in humans are

Corresponding author: Savio L.C. Woo, Ph.D., Department of Gene and Cell Medicine, Mount Sinai School of Medicine, One Gustave L. Levy Place, Box 1496, New York, New York 10029-6574. Fax: 212-803-6740. savio.woo@mssm.edu.

⁴Current address: 2nd Medical Department, Klinikum rechts der Isar, Technical University of Munich, Germany

generally asymptomatic or result in mild febrile illness.¹² VSV is not endemic to the North American population, implying that there will not be preexisting neutralizing antibodies or memory cellular immune responses in patients to interfere with its clinical application in the future.¹³

Hepatocellular carcinoma (HCC) is the third leading cause of cancer death and the fifth most common type of cancer in the world, accounting for over one million cases annually.¹⁻³ While the incidence of HCC has more than doubled over the last two decades,^{4, 5} the availability of curative treatment options remains extremely limited. Our group has previously described the efficacy of recombinant VSV as an oncolytic vector for treatment of HCC in the livers of immune-competent rats.¹⁴ We demonstrated that VSV, when administered at its maximum tolerated dose (MTD) via the hepatic artery, could gain access to and selectively replicate in multi-focal HCC tumors of various sizes, resulting in tumor necrosis and prolongation of animal survival.^{15, 16} Although encouraging, complete tumor regression and long-term survival were not observed in the treated animals as they eventually succumbed to relapse, highlighting the need for improvement of our treatment strategy.

While robust intratumoral virus replication was observed at one day post-vector administration, it was immediately followed by a logarithmic decline in subsequent days.¹⁵ Since the neutralizing anti-viral antibody response in the host is not effectively launched until at least day 5,¹⁶ we suspected that the drastic reduction in intratumoral virus titer after the first day is secondary to an anti-viral inflammatory response at the tumor sites. Cellular components of the innate immune system, such as granulocytes, NK cells, NKT cells and macrophages, have been demonstrated by others to be rapidly recruited and activated at sites of viral infection.¹⁸ These cells participate in the anti-viral response both by directly killing infected cells and by producing anti-viral cytokines. Thus we hypothesized that the host inflammatory response to VSV infection plays a critical role in suppression of intratumoral VSV replication, and counteracting these responses would substantially enhance VSV oncolysis and treatment efficacy.

Many inflammatory processes are mediated by chemo-attractant and immuno-modulatory molecules called chemokines,²¹ which play a central role in the host defense against invading viruses and in the pathogenesis of inflammatory diseases.^{22, 23} A number of viruses have evolved elegant mechanisms to evade detection and subsequent destruction by various immune cells in the host.²⁴ One such mechanism involves the production of secreted chemokine binding proteins, which exhibit no sequence homology to any known host proteins, yet function to competitively bind and/or inhibit the interactions of chemokines with their cognate receptors,²⁵ thereby suppressing the chemotaxis of inflammatory cells to the infection sites. While the functions and mechanisms of viral chemokine binding proteins (vCKBPs) have been extensively studied, they had not been exploited for the purpose of enhancing the oncolytic potency of heterologous viruses for cancer treatment. We report here the molecular construction and characterization of a novel rVSV vector which encodes the secreted form of the equine herpesvirus-1 glycoprotein G, which is a vCKBP which binds C, CC, and CXC chemokines with high affinity.²⁶ The rVSV vector was shown to block NK cell migration to the tumor sites, which permitted greatly enhanced intratumoral virus replication that led to elevated tumor necrosis and substantially prolonged survival of immune-competent rats bearing syngeneic and multi-focal HCC lesions in the livers.

RESULTS

Logarithmic elevation of intratumoral VSV titer and enhanced tumor response with antibody-mediated NK cell depletion in HCC-bearing rats

To evaluate the role of NK cells in suppressing intratumoral VSV replication, HCC-bearing rats were treated with PBS or rVSV-F at 1.3×10^7 pfu/rat, in the presence of rabbit anti-asialoGM1 or a control rabbit antibody. Tumor tissues were obtained from animals sacrificed at day 3 post vector administration, and NK cells in tumor sections were identified by immunohistochemical staining (Fig. 1A). There were only few NK cells in the lesions of PBS-treated animals, with or without anti-asialoGM1 antibody depletion (frames a and b). Accumulation of NK cells at the lesions was evident after rVSV-F treatment (frame c), which was substantially reduced after anti-asialoGM1 antibody depletion (frame d). Lysates from frozen tumor tissues were subjected to TCID₅₀ assays. While there were no detectable VSV titers in tumor extracts of PBS-treated animals, intratumoral virus titers in rVSV-F treated rats were elevated by 1–2 logs with anti-asialoGM1 administration (Fig. 1C, $p=0.002$). Liver sections containing tumors were obtained for histological staining (Fig. 1B), and there were few areas of spontaneous necrosis in the tumors of PBS-treated animals (frames a and b). Substantial necrotic areas were observed in tumors after rVSV-F treatment (frame c), which were significantly enhanced after anti-asialoGM1 administration (frame d). The percentage of necrosis within tumors was quantified by morphometric analysis, which revealed a substantial enhancement of tumor response to rVSV-F treatment with anti-asialoGM1 depletion than without (Fig. 1D, $p=0.002$). Collectively these results suggest that NK cells play a major role in suppressing intratumoral VSV replication that could be reversed by their depletion *in vivo*, which then led to substantially enhanced oncolysis and tumor response.

Construction and functional characterization of a rVSV vector expressing the equine herpesvirus-1 glycoprotein G

The equine herpesvirus-1 glycoprotein G (g_{EHV-1}) is a broad spectrum chemokine binding protein that suppresses the chemotaxis of inflammatory cells in response to C, CC and CXC chemokines with high affinity.²⁶ The cDNA corresponding to the secreted form of g_{EHV-1} was cloned into the full-length genome of VSV as a new transcription unit after the VSVG gene (Fig. 2A). The firefly luciferase gene (Luc) was inserted behind the g_{EHV-1} gene as a second translational unit under the control of the ubiquitously expressed EMCV internal ribosomal entry site (IRES). The corresponding rVSV vector (rVSV-gG) was rescued by reverse genetics as described previously^{27, 28}. To determine if the g_{EHV-1} protein expressed by rVSV-gG infected cells is functional, migration assays of NK cells in response to macrophage inflammatory protein-1 α (MIP-1 α), a CC chemokine, were performed in 24-well transwell plates. The results showed that NK cell migration was significantly inhibited by conditioned media from rVSV-gG infected rat HCC cells as compared to that from rVSV-F (Fig. 2B, $p=0.01$), indicating the recombinantly produced chemokine binding protein in infected rat HCC cells was functional. Additionally, virus replication and cell killing assays on rat HCC cells indicated that the rVSV-gG vector was equally effective as rVSV-F (results not shown).

Logarithmic elevation of intratumoral rVSV-gG titers and enhanced tumor response

To assess the *in vivo* effect of vector-mediated intratumoral g_{EHV-1} production on intratumoral virus replication and oncolysis, multi-focal HCC lesions were created via injection of rat HCC cells through the portal vein of male Buffalo rats as previously described¹⁵. Multi-focal lesions that ranged from 1–10 mm in diameters developed in their livers after 21 days, and they were treated with either PBS, 1.3×10^7 pfu of rVSV-gG, or rVSV-F via hepatic artery infusion. The animals were sacrificed on day 3 after treatment and tumor samples were collected and fixed for histological and immunohistochemical staining, as well as snap-frozen

for intratumoral virus titer quantification. Anti-VSVG antibody staining revealed the presence of viral membrane glycoprotein within tumors of rVSV-gG treated animals, which appeared more abundant than that observed in the rVSV-F and PBS treated rats (Fig. 3A, frames a–c). To quantify the virus yields in the lesions, lysates prepared from snap-frozen tumor samples from the treated animals were subjected to TCID₅₀ analysis. While rVSV-F infusion resulted in virus titers of less than 10⁴ TCID₅₀/mg of tumor tissue, rVSV-gG administration led to a one-log enhancement in intratumoral virus titer (Fig. 3B, p=0.04). To determine the impact of enhanced intratumoral replication of the rVSV-gG vector on tumor response, tumor-containing liver sections from the animals in the above experiment were examined by H & E staining (Fig. 3A, frames d–f), and the necrotic areas were quantified by morphometric analysis. A substantially enhanced response was observed in tumors of rats treated within the rVSV-gG vector over those treated with the rVSV-F vector (Fig. 3C, p=0.003). Additionally, the surrounding liver tissues to tumors were completely normal and without any evidence of pathology (results not shown).

Reduced accumulation of NK and NKT cells in tumors of rVSV-gG-treated rats

Multi-focal HCC-bearing Buffalo rats were treated with either PBS or 1.3×10⁷ pfu of rVSV-gG or rVSV-F via the hepatic artery. On day 3 after treatment, animals were sacrificed and tumor-containing liver sections were prepared for immunohistochemical staining of various immune cell types. Sections were stained for NK cells with anti-NKR-P1A (Fig.4A, frames a–c) and T cells by anti-OX-52 (Fig.4A, frames d–f). Semi-quantification of marker-positive cells using ImagePro software revealed that there was substantial accumulation of NK cells at the lesions after rVSV-F infusion over the PBS-treated rats (Fig.4C, p=0.04), which was substantially reduced after rVSV-gG treatment (Fig.4C, p=0.0004). There was also a statistically significant difference in the number of pan-T marker-positive cells after rVSV-gG infusion (Fig.4D, p=0.04). To determine whether these were NKT cells or T-lymphocytes, indirect immunofluorescence staining was performed. Consecutive tumor sections from rVSV-F-treated animals were stained with R-PE-conjugated mouse anti-rat CD3 antibody and FITC-conjugated mouse anti-rat NKR-P1A antibody, and the merged pictures indicate that the pan-T-positive cells present in the tumors were NKT cells rather than T-lymphocytes (Fig.4B, frames a–c). Collectively, the results indicate that NK and NKT cells were the effector inflammatory cells, and their chemotaxis to the tumor sites was substantially inhibited by vector-mediated expression of gG_{EHV-1}.

Substantial prolongation of survival of multi-focal HCC-bearing rats treated with rVSV-gG versus rVSV-F

To assess the potential of the rVSV vector expressing a vCKBP that inhibits NK and NKT cell chemotaxis as an oncolytic agent, rats bearing multi-focal HCC tumors in their livers were randomly assigned to receive either a single infusion of PBS (n=8), 1.3×10⁷ pfu of rVSV-gG (n=15), or an equal dose of the rVSV-F vector (n=10) via the hepatic artery, and the animals were monitored daily for survival (Fig. 5). While all animals in the PBS or rVSV-F treatment groups expired by day 21 or 29, respectively, rVSV-gG treatment resulted in a highly significant prolongation of survival (P=0.00001), with 5 of 15 animals (33%) achieving survival of 150 days. The long-term surviving rats in this treatment group were sacrificed on day 150 and evaluated for residual malignancy. Macroscopically and histologically, there was no detectable tumor within the liver or elsewhere. These results indicate that huge multi-focal lesions in the liver (up to 10mm in diameter at the time of oncolytic virus treatment) had undergone complete remission in these animals, which translated into long-term and tumor-free survival.

Apparent Lack of serum and organ toxicities after rVSV-gG administration in tumor-bearing rats

To critically evaluate if there were viremia and toxicities in tumor-bearing rats after administration with rVSV-gG versus rVSV-F at the effective dose, blood samples were taken at one day before virus infusion (D-1) and at 30 minutes (D0), one (D1), three (D3), seven (D7) and fourteen (D14) days after virus administration. Virus titers were determined by TCID50 assays in BHK-21 cells. Serum virus titers in rats treated with both rVSV-gG and rVSV-F were highest at D0, which were followed by logarithmic declines after one day to undetectable levels after seven days (mean \pm standard deviation, n=5 for each group at each time point), indicating that there was no viremia after intraarterial administration of either vector (Fig. 6A). To assess systemic toxicity, we monitored blood chemistries in rVSV-gG and rVSV-F treated rats. No difference was detected in the levels of WBC, RBC, hemoglobin, hematocrit, urea nitrogen and creatinine, all of which remained within the respective normal ranges at all time points (Fig. 6B). Serum transaminases were significantly elevated in the rats before vector treatment, indicative of the fact that these are HCC-bearing animals. There was a peak of serum transaminase levels at one day after either vector administration that could be attributed to VSV-induced oncolysis of HCC cells and subsequent release of transaminases into the circulation (Fig. 6B). Importantly, the elevated transaminase levels were comparable between two vector-treated groups, which returned to the pre-treatment level after three days. To assess proinflammatory response, serum levels of IL6, TNF- α and IFN- γ were monitored. There were no detectable levels of serum TNF- α (<12.5 pg/ml) and IFN- γ (<31.2 pg/ml) in the rVSV-F and rVSV-gG treated rats at all time points (results not shown). Although there was a slight but statistically significant elevation of serum IL6 in rVSV-gG, but not rVSV-F, treated rats from 60 pg/ml to 120 pg/ml at D0, the peak was more than two logs below concentrations associated with systemic toxicity and returned to normal after one day (Fig. 6B). The animals were sacrificed at day 14 and the major organs including the liver, heart, lung, kidney, spleen, duodenum, brain and spinal cord were harvested for macroscopic and histological examination. All tissues appeared normal with no signs of pathology (results not shown). The results indicated that hepatic arterial administration of rVSV-gG at the effective dose did not induce viremia or systemic and organ toxicities in HCC-bearing rats.

DISCUSSION

In the present study, we have focused on the development of a novel rVSV vector that encodes a vCKBP from a heterologous virus as an effective and safe oncolytic agent to treat multi-focal HCC in an immune-competent animal model. We provide evidence that the treatment efficacy of rVSV-F can be greatly enhanced by depletion of NK cells in tumor-bearing rats by administration of a rabbit anti-asialoGM1 antibody, and that rVSV-gG possesses greatly elevated oncolytic potency over rVSV-F, which translates into substantially enhanced tumor response and highly significant prolongation of survival.

Although our previous studies have shown that rVSV vector administration via the hepatic artery in multi-focal HCC tumor-bearing rats resulted in efficient tumor-selective virus replication, oncolysis and survival prolongation,^{15–17,29} intratumoral virus replication peaked at only one-day post vector administration that led to a limited tumor response, leaving behind a wide border of viable tumor cells that caused tumor relapse in most treated animals. Since neutralizing antibodies to VSV were not detected in the rats until day 5 post vector injection,^{15–17} we hypothesized that the logarithmic decline in intratumoral virus replication at the early phase of infection was mediated by anti-viral inflammatory cells that accumulated in the lesions after 1–2 days, and that suppression of these inflammatory cell migration to the tumor sites would lead to substantially enhanced intratumoral virus replication, which was verified by *in vivo* depletion of NK cells in tumor-bearing rats using anti-asialoGM1 antibody. We further

hypothesized that suppression of chemotaxis of anti-viral inflammatory cells can be achieved by genetic modification of the rVSV genome to express heterologous viral chemokine binding proteins, which will in turn lead to elevated VSV-mediated oncolysis, tumor response and substantial survival prolongation. In this study, we tested the hypothesis by constructing a rVSV vector encoding the secreted form of glycoprotein G from equine herpes virus-1, which has demonstrated vCKBP activity and binds a broad range of chemokines with high affinity.²⁶ The g_{EHV-1} protein blocks chemokine activity by preventing their interactions with specific receptors and glycosaminoglycans, which is a required interaction for the correct presentation and function of chemokines. The g_{EHV-1} protein is therefore an excellent candidate for vector-mediated suppression of host anti-viral inflammatory responses to enhance the oncolytic potency of VSV, which was proven to be the case experimentally.

To define the effect of the genetically modified rVSV vector expressing g_{EHV-1}, in terms of its ability to evade the host antiviral immune response and allow unrestrained viral replication and cell killing within HCC tumors, it was important to test the vector in tumor-bearing animals. On day 3 after treatment by hepatic artery infusion, positive staining for VSVG protein was indeed augmented within tumors of rats treated with rVSV-gG as compared to the control rVSV-F vector, and intratumoral virus titers increased by one-log. Furthermore, rVSV-gG treatment resulted in significantly enhanced tumor necrosis. To examine the mechanism whereby expression of g_{EHV-1} resulted in substantially elevated intratumoral rVSV titers, we performed immunohistochemical staining of various immune cell types in tumor sections from animals treated with PBS, rVSV-gG, or rVSV-F. Interestingly, natural killer cells seemed to be the major immune cell type recruited in response to rVSV-F infection. rVSV-gG treatment resulted in an inhibition of NK and pan-T positive cells within tumors. Subsequent immunofluorescence studies identified the pan-T positive cells recruited in response to rVSV-F infection as NKT cells.

Natural killer cells are a major component of the innate immune system, and are crucial in early defense against viral infection.³⁰ These cells represent a distinct population of cytotoxic lymphocytes that act as a first line of defense against invading viruses as an integral component of the innate cellular immune response system, prior to the launch of the adaptive immune responses.^{31–33} NK cells are activated during viral infections,³⁴ and they mediate direct lysis of target cells by releasing cytotoxic granules containing lytic enzymes, or by binding to apoptosis-inducing receptors on the target cell.^{35, 36} Interestingly, an *in vitro* study demonstrated that NK cells preferentially lyse human colon adenocarcinoma (Colo-205) tumor cells infected with herpes simplex virus type 1 and vaccinia virus at an early stage of infection, thereby preventing viral dissemination to neighboring cells.³³ These data are consistent with our observation that inhibition of NK cells through the expression of a vCKBP with NK inhibitory function resulted in enhanced VSV replication in the tumors. The second type of inflammatory cells inhibited by rVSV-gG was identified as NKT cells through immunofluorescent analysis. NKT cells are a subset of NK cells, found within the T cell populations.³⁶ NKT cells represent a small percentage of T cells found in the thymus and spleen, but constitute a significant proportion of those in the liver.³⁷ Taken together, it might be postulated that the glycoprotein G from the alphaherpesviruses has evolved in such a way to evade the anti-viral assault by NK and NKT cells in order to promote its own propagation within the infected host. This vCKBP property of the g_{EHV-1} made it an excellent candidate for enhancement of the oncolytic potency of VSV.

A limitation to the above interpretation is the lack of direct evidence that the vector treatment led to intratumoral g_{EHV-1} expression *in vivo* due to a lack of specific antibody preparations to the viral chemokine binding protein, and g_{EHV-1} concentrations in tumor extracts were too low to be quantified by the NK cell migration assay *in vitro*. In the absence of these data, alternative mechanisms such as the direct infection and lysis of NK/NKT cells by the rVSV-

gG vector, gG-induced up-regulation of NKG2D ligands that causes NK cell death³⁸, elevated expression of MHC-I in tumor cells³⁹ and TLR on dendritic cells⁴⁰ should also be considered. Additionally, the role of cellular immunity has been described in other oncolytic virus systems, particularly with respect to NK cells, T cells and macrophages. Interestingly, there is evidence to suggest that these cells can augment the tumoricidal effects of oncolytic HSV as virus infection of tumor cells elicits a robust adoptive anti-tumor immune response^{41–43}. These seemingly contradictory results from the current studies could be reconciled by the fact that NK cells have multiple functions in immune-competent animals. First, it is known to be an integral component of the innate cellular immune response system that kill virus-infected cells directly and it is this function that is attenuated by the viral chemokine binding proteins. Another function of NK cells is to augment an adoptive immune response against cells expressing viral antigens, which has been documented in the oncolytic HSV literature.

Finally, while it is important to develop recombinant oncolytic virus vectors with greater potency for cancer treatment, strategies focused on inhibition of key players in antiviral defenses could be construed as a potentially dangerous proposition in the development of therapeutic agents for future clinical application. To address this concern, we demonstrated in immune-competent tumor-bearing rats that the rVSV-gG vector introduced no additional toxicities compared to the rVSV-F vector, despite the fact that expression of g_{GEHV-1} inhibited the chemotaxis of NK and NKT cells to virus-infected lesions. This is most likely to be secondary to the exquisite sensitivity of VSV to type I interferon response in normal cells,¹¹ which is unaltered in the vCKBP-expressing vectors. In conclusion, we have presented a novel rVSV vector, which exploits the anti-inflammatory activities of a broad-spectrum chemokine binding protein. This vector demonstrates superior intratumoral replication, oncolysis, and prolongation of survival in multi-focal HCC tumor-bearing rats, while maintaining the same safety profile as the other rVSV vectors. Thus, rVSV vectors encoding vCKBPs have the potential for development into effective and safe therapeutic agents for the treatment of HCC and possibly other types of cancer in the future. Furthermore, since anti-viral inflammatory responses are key components in the host's defense against invading pathogens, the concept and technology developed here might be generally applicable in substantially enhancing the potency of other oncolytic virus agents without inherent anti-inflammatory activities.

EXPERIMENTAL PROCEDURES

Cell lines

BHK-21 cells and rat McA-RH7777 cells were purchased from the American Type Culture Collection (Manassas) and maintained in Dulbecco's Modified Eagle Medium (Mediatech). All culture media were supplemented with 10% heat-inactivated fetal bovine serum (Sigma-Aldrich) and 100U/ml penicillin-streptomycin (Mediatech).

Plasmid construction and vector rescue

The rVSV vector expressing a mutant (L289A) NDV fusion protein (rVSV-F) was previously described¹⁶. To create a rVSV vector expressing the secreted form of g_{GEHV-1} a truncated gene (1–1065 bp) as determined by hydrophobicity plotting was synthesized chemically in its entirety (GenScript, Piscataway, NJ), which is consistent with the findings of others.²⁶ To generate a plasmid simultaneously expressing g_{GEHV-1} and firefly Luciferase, the ubiquitously expressed ECMV internal ribosomal entry site (IRES) was introduced so that the two genes could be co-translated as a single transcriptional unit. Sequencing of the plasmids was conducted in the DNA Sequencing Core Facility at Mount Sinai School of Medicine. To rescue the recombinant VSV vector, the established method of reverse genetics was employed^{27, 28} and their titers were determined by plaque assays on BHK-21 cells.

Multi-focal HCC model and animal studies

All procedures involving animals were approved by and performed according to the guidelines of the Institutional Animal Care and Use Committee of the Mount Sinai School of Medicine. Six-week old male Buffalo rats were purchased from Harlan and housed in a pathogen-free environment. To establish multifocal HCC lesions within the liver, 10^7 syngeneic McA-RH7777 rat HCC cells were infused into the portal vein. 21 days after tumor cell implantation, 1.3×10^7 pfu of VSV or PBS in 1 ml were administered via the hepatic artery. To evaluate tumor response, animals were sacrificed 3 days after infusion and tumors were subjected to histological, immunohistochemical and immunofluorescent staining, as well as TCID₅₀ analysis of tumor extracts. In addition, groups of animals infused with VSV vectors or PBS were followed for survival.

In vivo NK cells depletion

NK cell depletion in tumor-bearing rats was accomplished by intravenous administration of 1 mg/rat of a polyclonal rabbit anti asialo GM1 antibody (Wako Chemical USA, Inc.), or normal rabbit serum (control Ig), at 24 hours before and after rVSV-F infusion and the animals were sacrificed on day 3 after rVSV-F treatment.

Histology and immunohistochemistry

Liver samples containing tumor were fixed overnight in 4% paraformaldehyde and then paraffin-embedded. Thin sections were subjected to either H&E staining for histological analysis or immunohistochemical staining using monoclonal antibodies against VSVG protein (Alpha Diagnostic) or myeloperoxidase (Abcam). Another set of liver samples containing tumor were fixed overnight 4% paraformaldehyde and then equilibrated in 20% sucrose in PBS overnight. Frozen sections were subjected to immunohistochemical staining using monoclonal antibodies against NKR-P1A (BD Pharmingen), OX-52 (BD Pharmingen), or ED-1 (Chemicon). Semi-quantification of positively stained cells was performed using ImagePro Software (Media Cybernetics Inc), and immune cell index was calculated as a ratio of positive cell to unit tumor area (10,000 pixels as one unit tumor area). Additionally, frozen sections were fixed with cold acetone and blocked with 4% goat serum, followed by staining with R-PE-conjugated mouse anti-rat CD3 monoclonal antibody (BD Pharmingen) and FITC-conjugated mouse anti-rat NKR-P1A antibody (BD Pharmingen). Nuclear DNA was stained with DAPI.

Assessment of Serum Virus Titer, Proinflammatory Cytokine Production, Complete Blood Count (CBC) and Serum Chemistry

Multifocal HCC tumor-bearing rats were given either rVSV-F or rVSV-gG at the effective dose. Blood samples were collected from the tail vein at one day before (D-1) and at 30 minutes (D0), one (D1), three (D3), seven (D7) and fourteen (D14) days after vector infusion. Infectious virus titers were determined by TCID₅₀ assay in BHK-21 cell and the levels of serum proinflammatory cytokines were determined by ELISA (Biosource, Camarillo, CA, USA). CBC as well as serum chemistry including Hemoglobin, Hemocrit, ALT, AST, BUN and creatinine were performed at the Chemistry Laboratory at Mount Sinai School of Medicine.

Statistical analyses

For comparison of individual data points, two-sided student t-test was applied to determine statistical significance. Survival curves of animals were plotted according to the Kaplan-Meier method, and statistical significance in different treatment groups was compared using the log-rank test. Results and graphs were obtained using the GraphPad Prism 3.0 program (GraphPad Software).

Acknowledgments

The work was supported in part by a NIH grant (CA100830 to SLCW), the German Cancer Aid (Max-Eder Research Program) and a Federal Ministry of Education and Research Grant 01GU0505 to OE. We thank Drs. Tian-gui Huang and Luis Martinez-Sobrido for helpful discussions, Dr. John Fallon for consultation on histological and immunohistochemical analyses of tissue samples, and Ms. Sonal Harbaran and Ms. Yafang Wang for excellent technical assistance. For disclosure of financial conflicts of interest, the work forms the scientific basis of a patent application, of which JA, OE, AG and SW are co-inventors.

REFERENCES

1. Parkin DM, Sthernsward J, Muir CS. Estimates of the worldwide frequency of twelve major cancers. *Bull World Health Organ* 1984;62:163–182. [PubMed: 6610488]
2. Murray CJ, L AD. Evidence-based health policy - lessons from the Global Burden of Disease Study. *Science* 1996;274:740–743. [PubMed: 8966556]
3. Parkin DM, Bray F, Ferlay J, Pisani P. Estimating the world cancer burden: Globocan 2000. *Int J Cancer* 2001;94:153–156. [PubMed: 11668491]
4. El-Serag HB, M AC. Rising incidence of hepatocellular carcinoma in the United States. *N Engl J Med* 1999;340:745–750. [PubMed: 10072408]
5. Dyer Z, Peltekian K, van Zanten SV. The changing epidemiology of hepatocellular carcinoma in Canada. *Aliment Pharmacol Ther* 2005;22:17–22. [PubMed: 15963075]
6. Yeung YP, Lo CM, Liu CL, et al. Natural history of untreated nonsurgical hepatocellular carcinoma. *Am J Gastroenterol* 2005;100:1995–2004. [PubMed: 16128944]
7. Kirn D, Martuza RL, Zwiebel J. Replication-selective virotherapy for cancer: biological principles, risk management, and future directions. *Nat Med* 2001;7:781–787. [PubMed: 11433341]
8. Coffey MC, Strong JE, Forsyth PA, Lee PW. Reovirus therapy of tumors with activated Ras pathway. *Science* 1998;282:1332–1334. [PubMed: 9812900]
9. Lorence RM, Katubig BB, Reichard KW, et al. Complete regression of human fibrosarcoma xenografts after local Newcastle disease virus therapy. *Cancer Research* 1994;54:6017–6021. [PubMed: 7954437]
10. Peng KW, Ahmann GJ, Pham L, et al. Systemic therapy of myeloma xenografts by an attenuated measles virus. *Blood* 2001;98:2002–2007. [PubMed: 11567982]
11. Stojdl DF, Lichty B, Knowles S, Marius R, Atkins H, Sonenberg N, Bell JC. Exploiting tumor-specific defects in the interferon pathway with a previously unknown oncolytic virus. *Nat Med* 2000;6:821–825. [PubMed: 10888934]
12. Letchworth GJ, Rodriguez LL, Del C, Barrera J. Vesicular Stomatitis. *Vet J* 1999;157:239–260. [PubMed: 10328837]
13. Rose, JK.; Whitt, MA. *Fields Virology*. Edn. 4th. Knipe, DM.; Howley, PM., editors. Lippincott Williams & Wilkins; Philadelphia: 2001. p. 1221-1242.
14. Ebert O, Shinozaki K, Huang TG, Savontaus MJ, Garcia-Sastre A, Woo SLC. Oncolytic vesicular stomatitis virus for treatment of orthotopic hepatocellular carcinoma in immune-competent rats. *Cancer Research* 2003;63:611–613.
15. Shinozaki K, Ebert O, Kournioti C, et al. Oncolysis of multifocal hepatocellular carcinoma in the rat liver by hepatic artery infusion of vesicular stomatitis virus. *Mol Ther* 2004;9:368–376. [PubMed: 15006603]
16. Ebert O, Shinozaki K, Kournioti C, et al. Syncytia induction enhances the oncolytic potential of vesicular stomatitis virus in virotherapy for cancer. *Cancer Research* 2004;64:3265–3270. [PubMed: 15126368]
17. Shinozaki K, Ebert O, Suriawinata A, Thung S, Woo S. Prophylactic alpha interferon treatment increases the therapeutic index of oncolytic vesicular stomatitis virus virotherapy for advanced hepatocellular carcinoma. *J Virol* 2005;79:13705–13713. [PubMed: 16227290]
18. Guidotti LG, C FV. Noncytolytic control of viral infections by the innate and adaptive immune response. *Annual Review of Immunology* 2001;19:65–91.
19. Wakimoto H, Johnson PR, Knipe DM, et al. Effects of innate immunity on herpes simplex virus and its ability to kill tumor cells. *Gene Therapy* 2003;10:983–990. [PubMed: 12756419]

20. Wakimoto H, Fulci G, Tuminiski E, et al. Altered expression of antiviral cytokine mRNAs associated with cyclophosphamide's enhancement of viral oncolysis. *Gene Therapy* 2004;11:214–223. [PubMed: 14712306]
21. Schall TJ, Bacon KB. Chemokines, leukocyte trafficking, and inflammation. *Curr. Opin. Immunol* 1994;6:865–873. [PubMed: 7710711]
22. Rollins BJ. Chemokines. *Blood* 1997;90:909–928. [PubMed: 9242519]
23. Baggiolini M. Chemokines and leukocyte traffic. *Nature* 1998;392:565–568. [PubMed: 9560152]
24. Alcami A. Viral mimicry of cytokines, chemokines, and their receptors. *Nature Immunology* 2003;3:36–50.
25. Seet B, McFadden G. Viral chemokine-binding proteins. *Journal of Leukocyte Biology* 2002;72:24–34. [PubMed: 12101259]
26. Bryant NA, Davis-Poynter N, Vanderplasschen AI, et al. Glycoprotein G isoforms from some alphaherpesviruses function as broad-spectrum chemokine binding proteins. *Embo J* 2003;22:833–846. [PubMed: 12574120]
27. Lawson ND, Stillman EA, Whitt MA, et al. Recombinant vesicular stomatitis viruses from DNA. *Proc. Natl. Acad. Sci* 1995;92:4477–4481. [PubMed: 7753828]
28. Whelan SP, Ball LA, Barr JN, et al. Efficient recovery of infectious vesicular stomatitis virus entirely from cDNA clones. *Proc. Natl. Acad. Sci* 1995;92:8388–8392. [PubMed: 7667300]
29. Shinozaki K, Ebert O, Woo SL. Eradication of advanced hepatocellular carcinoma in rats via repeated hepatic arterial infusions of recombinant VSV. *Hepatology* 2005;41:196–203. [PubMed: 15619242]
30. Trinchieri G. Biology of natural killer cells. *Adv Immunol* 1989;47:187. [PubMed: 2683611]
31. Welsh RM. Regulation of virus infections by natural killer cells. *Nat Immun Cell Growth Reg* 1986;5:169–199.
32. Brutkiewicz RR, Welsh RM. Major histocompatibility complex class I antigens and the control of viral infections by natural killer cells. *J Virol* 1995;69:3967–3971. [PubMed: 7769654]
33. Baraz L, Khazanov E, Condiotti R, Kotler M, Nagler A. Natural killer (NK) cells prevent virus production in cell culture. *Bone Marrow Transplantation* 1999;24:179–189. [PubMed: 10455347]
34. Biron CA, Nguyen KB, Pien GC, Cousens LP, Salazar-Mather TP. Natural killer cells in antiviral defense: function and regulation by innate cytokines. *Annual Review of Immunology* 1999;17:189–220.
35. Orange JS, Fassett MS, Koopman LA, et al. Viral evasion of natural killer cells. *Nature Immunology* 2002;3:1006–1012. [PubMed: 12407408]
36. Biron CA, Brossay L. NK cells and NKT cells in innate defense against viral infections. *Current Opinion in Immunology* 2001;13:458–464. [PubMed: 11498302]
37. Eberl G, Lees R, Smiley ST, Taniguchi M, Grusby MJ, MacDonald HR. Tissue-specific segregation of CD1d-dependent and CD1d-independent NK T-cells. *J Immunol* 1999;162:6410–6419. [PubMed: 10352254]
38. Mistry AR, O'Callaghan CA. Regulation of ligands for the activating receptor NKG2D. *Immunology* 2007;121:439–447. [PubMed: 17614877]
39. Nair DT, Kaur KJ, Singh K, Mukherjee P, Rajagopal D, George A, Bal V, Rath S, Rao KV, Salunke DM. Mimicry of native peptide antigens by the corresponding retro-inverso analogs is dependent on their intrinsic structure and interaction propensities. *J Immunol* 2003;170:1362–1373. [PubMed: 12538696]
40. Lund JM, Alexopoulou L, Sato A, Karow M, Adams NC, Gale NW, Iwasaki A, Flavell RA. Recognition of single-stranded RNA viruses by Toll-like receptor 7. *Proc Natl Acad Sci U S A* 2004;101:5598–5603. [PubMed: 15034168]
41. Todo T, Martuza RL, Rabkin SD, Johnson PA. Oncolytic herpes simplex virus vector with enhanced MHC class I presentation and tumor cell killing. *Proc Natl Acad Sci U S A* 2001;98:6396–6401. [PubMed: 11353831]
42. Thomas DL, Fraser NW. HSV-1 therapy of primary tumors reduces the number of metastases in an immune-competent model of metastatic breast cancer. *Mol Ther* 2003;8:543–551. [PubMed: 14529826]

43. Benencia F, Courreges MC, Conejo-Garcia JR, Buckanovich RJ, Zhang L, Carroll RH, Morgan MA, Coukos G. Oncolytic HSV exerts direct antiangiogenic activity in ovarian carcinoma. *Hum Gene Ther* 2005;16:765–778. [PubMed: 15960607]

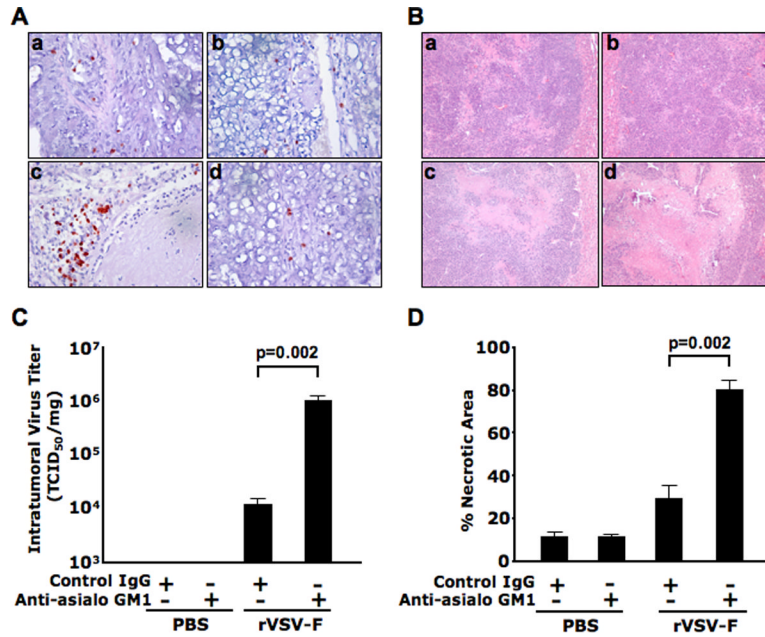


Figure 1. Logarithmic elevation of intratumoral rVSV replication and enhanced tumor necrosis by antibody-mediated depletion of NK cells in tumor-bearing rats
 Buffalo rats harboring multi-focal HCC lesions in the liver were intravenously injected with polyclonal antibodies anti-asialoGM1 (Wako, Richmond, VA) or control rabbit IgG at 1mg/200 μ l/rat at one day before rVSV-F infusion through the hepatic artery. A single injection of rVSV-F at 1.3×10^7 pfu/ml/rat or PBS was performed on the following day. The antibody injections were repeated via at one day after rVSV-F or PBS infusion (N=3 for each group). The treated animals were sacrificed 3 days after virus administration. Panel A shows the representative sections after immunohistochemical staining for NK cells in the four treatment groups (frame a, PBS with control rabbit IgG; frame b, PBS with anti-asialoGM1; frame c, rVSV-F with control rabbit IgG and frame d, rVSV-F with anti-asialoGM1). Panel B shows the representative sections after H&E staining in the same treatment groups as described in panel A above. Panel C shows viral titers from tumor lysates, expressed in TCID₅₀ per mg of tumor tissue. Viral titers following treatment with rVSV-F + control Ig versus rVSV-F + Anti-asialoGM1 were statistically significant by unpaired T-test analysis ($p=0.002$). Panel D shows percentages of necrotic areas within tumors, as quantified by morphometric analysis of H&E-stained tumor sections. Percentages of necrosis in tumors from animals treated with rVSV-F + control Ig were compared with those treated with rVSV-F + Anti-asialoGM1 by unpaired T-test ($p=0.002$).

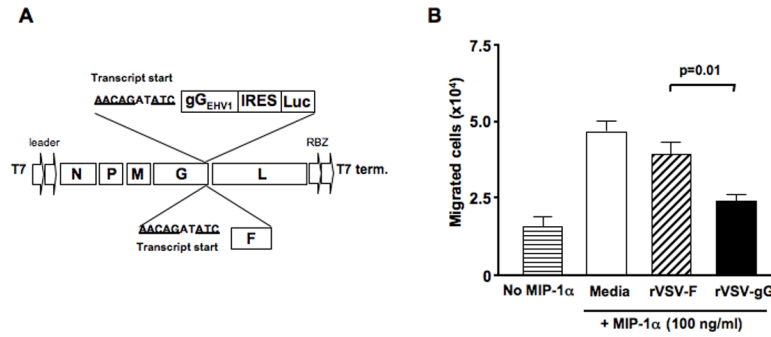


Figure 2. Molecular construction, rescue and functional characterization of rVSV-gG in vitro
 Panel A, a schematic representation of rVSV-F and rVSV-gG. The full-length pVSV plasmid containing five transcription units, and a bicistronic construct containing the Equine Herpesvirus 1 gG (gG_{EHV1}) and firefly luciferase (Luc), with an intervening IRES from EMCV, are shown. The transgenes are preceded by a VSV transcription termination signal, an intergenic region and a transcription start signal, and are inserted into the 3'-untranslated region of the VSVG gene. Panel B, inhibition of NK cell migration in response to MIP-1 α by conditioned media from rVSV-gG infected rat HCC cells. The NK cell migration assays were performed using 24-well transwell plates. The migration of rat NK cells from the upper chamber to the lower chamber in response to 100ng/ml of MIP-1 α was monitored in the presence of ultra-filtered and UV-irradiated supernatants from 10⁵ HCC cells infected with rVSV-gG or rVSV-F. The number of NK cells in the lower chamber was counted after an incubation period of 4 hours at 37 degrees. Data presented are the mean values of four independent experiments and the results were analyzed statistically by two-sided student t test.

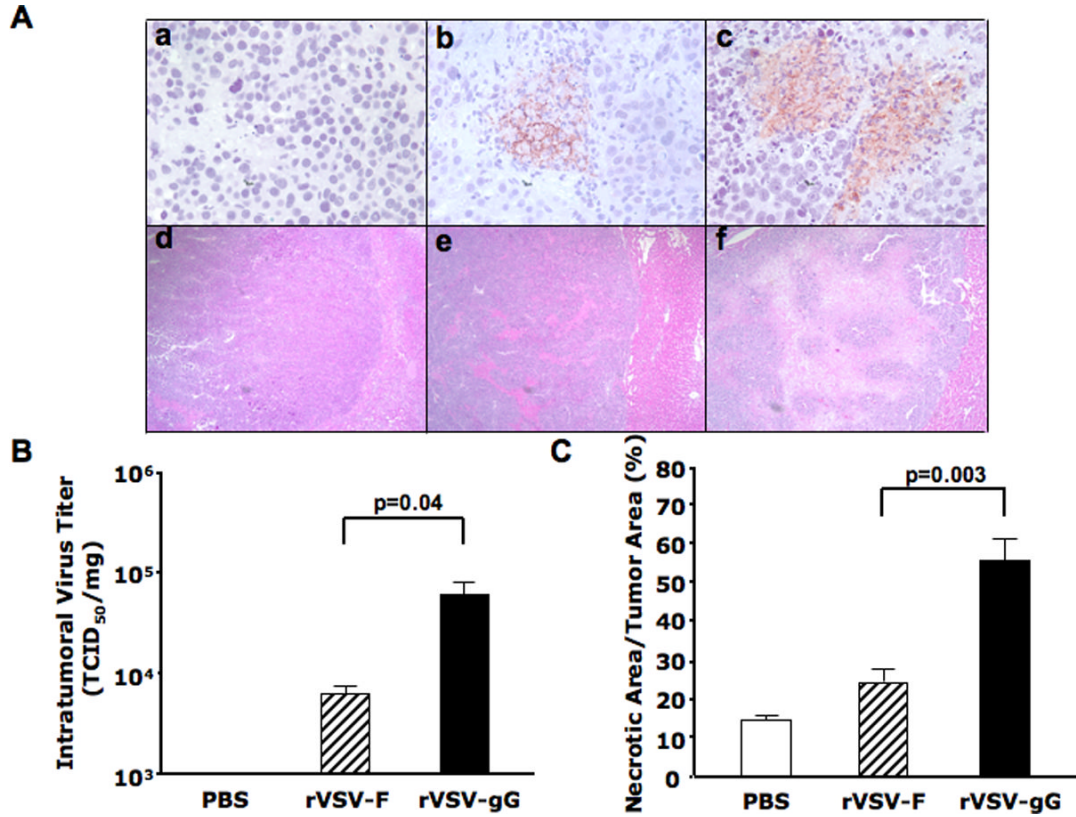


Figure 3. Intratumoral virus replication and tumor response in rats treated with rVSV-gG versus rVSV-F

Multi-focal HCC-bearing Buffalo rats were injected with PBS (n=3), rVSV-F (n=4) or rVSV-gG (n=4) at 1.3×10^7 pfu/ml/rat and sacrificed 3 days post-virus administration via hepatic artery. Panel A, tumor sections were stained with a monoclonal anti-VSVG antibody (frames a–c) or with H&E (frames d–f). Representative sections from rats treated with PBS (frames a and d), rVSV-F (frames b and e) and rVSV-gG (frames c and f) are shown (magnification=40×). Panel B, virus titers in tumor extracts on BHK-21 cells. Viral titers are expressed as TCID₅₀/mg tissue (mean + standard deviation), and the results were analyzed statistically by two-sided student t test (p=0.04). Panel C, tumor response as quantified by morphometric analysis using the ImagePro software. Data were shown as mean + standard deviation, and the results were analyzed statistically by two-sided student t test (p=0.003).

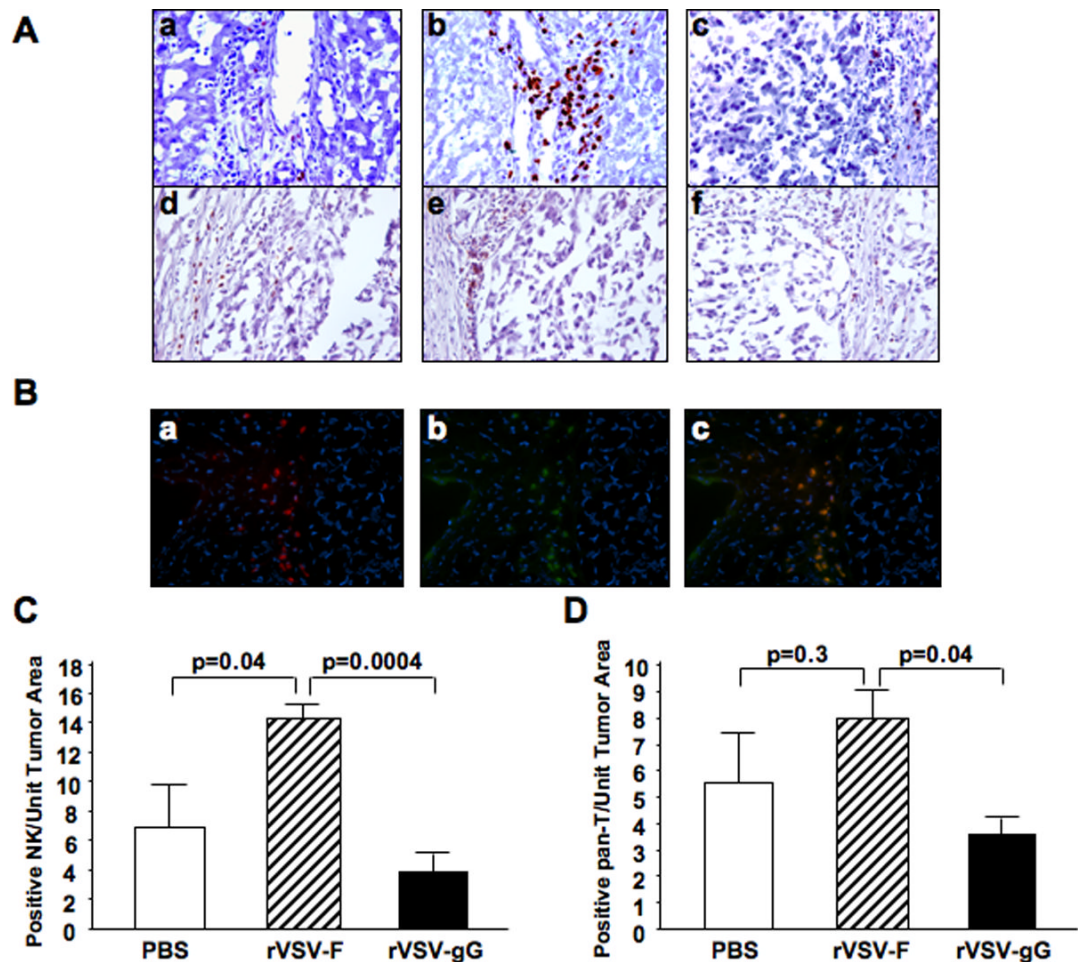


Figure 4. Immunohistochemical and immunofluorescent staining of NK and T cells in tumors of rats treated with rVSV-F versus rVSV-gG
 Panel A, representative immunohistochemically stained sections from tumors and surrounding tissues. Tumor-bearing rats were infused with PBS (frames a and d), rVSV-F (frames b and e) or rVSV-gG (frames c and f) at 1.3×10^7 pfu/ml/rat. Samples were obtained from rats at day 3 after virus infusion into the hepatic artery. Sections were stained with mouse monoclonal anti-NKR-P1A (frames a–c) or monoclonal anti-OX-52 (frames d–f) (magnification=40 \times). Panel B, representative immunofluorescent sections of rVSV-F infected rat HCC tumors. Frozen sections were fixed with cold acetone and blocked with 4% goat serum, followed by staining with R-PE-conjugated mouse anti-rat CD3 monoclonal antibody (frame a), FITC-conjugated mouse anti-rat NKR-P1A (frame b), and a merged picture (frames c) (magnification=40 \times). Panels C and D, semi-quantification of NK and T cells in the lesions after PBS, rVSV-F and rVSV-gG treatment, respectively, as quantified by morphometric analysis using the ImagePro software. Immune cell index was calculated as ratio of positive cell to unit tumor area (10,000 pixel as one unit tumor area), and the results were analyzed statistically by two-sided student t test.

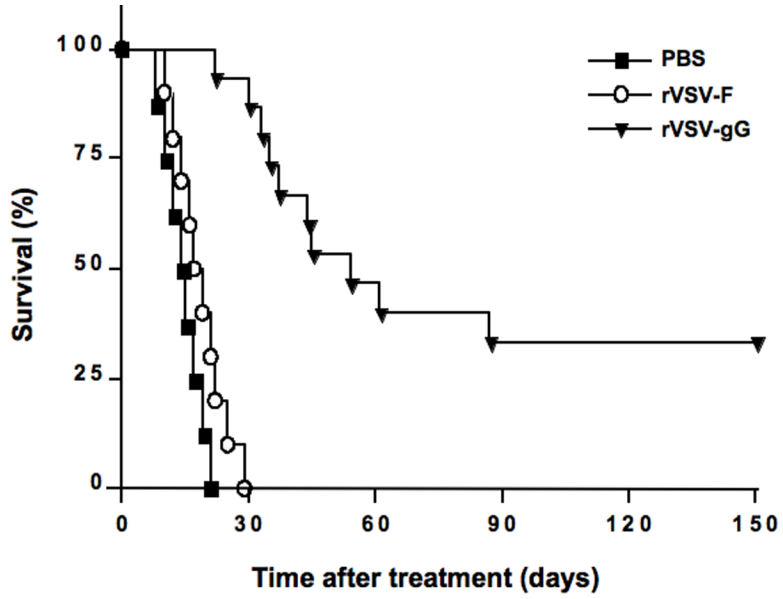


Figure 5. Kaplan-Meier survival curve of multi-focal HCC-bearing rats after rVSV-F versus rVSV-gG treatment
HCC-bearing rats were given hepatic arterial infusion of PBS (n=8), rVSV-F (n=10) or rVSV-gG (n=15) at 1.3×10^7 pfu/ml/rat. Survival was monitored daily and the results were analyzed statistically by log rank test ($p=0.00001$).

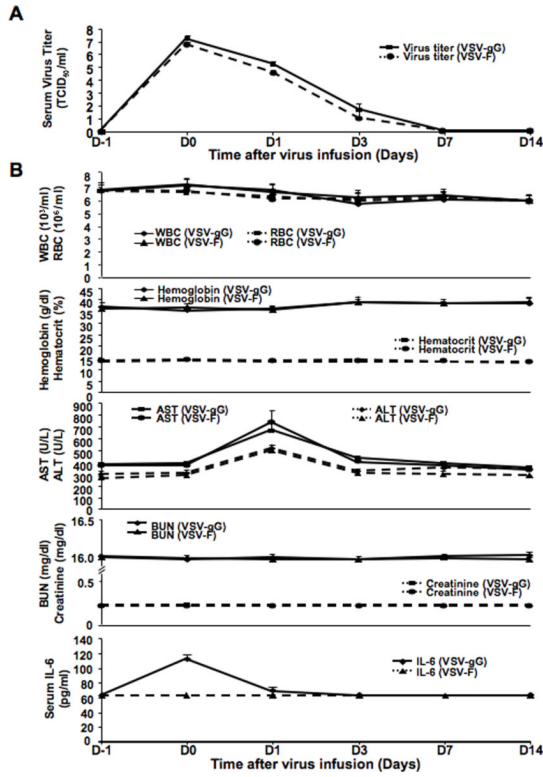


Figure 6. Toxicology studies of tumor-bearing rats after rVSV-gG and rVSV-F administration
 Panel A, kinetic profile of infectious virus yields in sera of tumor-bearing rats after infusion of rVSV-gG and rVSV-F. Virus titers (TCID₅₀/ml) in sera obtained from tumor-bearing animals at one day before (D-1), and at 30 minutes, 1, 3, 7 and 14 days after (D0, D1, D3, D7 and D14, respectively), virus infusion into hepatic artery are shown (mean ± standard deviation; n=4–5/time point). A peak of virus titer was observed at D0 for both vectors, which declined logarithmically to undetectable levels at D7 and thereafter. Panel B, determination of CBC and serum chemistries in tumor-bearing rats after hepatic arterial infusion of rVSV-gG and rVSV-F. Blood samples were collected from the same sets of animals as in Panel A at the indicated time points. WBC, RBC, hemoglobin, hematocrit, BUN and creatinine levels in the animals remained within their respective normal ranges at all time points after administration of either vector. Serum IL-6 levels in either vector treated rats were also below its detection limit (<62.5 pg/ml) at all time points, except at D0 (~120 pg/ml) in the rVSV-gG treated rats, although the peak was more than two orders of magnitude below that considered to be toxic.